Chiral symmetry, Conformal breaking, and transport coefficients in the two-flavour PNJL theory

Jingxu Wu[1,6] Yuwei Yin[2,6] Chenjia Li[1,6] Jiaming Chen[3,6]
Yifan He[4,5,6] Wenze Wang[3,6]

[1]Faculty of Physics, Lomonosov Moscow State University
[2]Department of Physics, École Polytechnique, Palaiseau, France
[3]Faculty of Mechanics and Mathematics , Lomonosov Moscow State University
[4]Department of Physics, Lanzhou University
[5]Lanzhou Center for Theoretical Physics
[6]GeZhi Theoretical Physics Reading Group

July 2025
Based on arXiv:2504.18567v1 [physics.gen-ph]

Outline

QCD Matter: Phases and Symmetries

- Thermodynamics of QCD is controlled by temperature T and baryon chemical potential μ_B.
- Two limiting regimes:
  - **Hadronic phase**: confinement + spontaneous chiral symmetry breaking (SχSB).
  - **Quark–Gluon Plasma (QGP)**: deconfinement + (approx.) restored chiral symmetry.
- Lattice QCD at small μ_B shows a smooth crossover near $T_c \sim 155\,\text{MeV}$; a first-order line and a critical end point (CEP) may appear at larger μ_B.

QCD Lagrangian and Global Symmetries

$$\mathcal{L}_{\text{QCD}} = -\frac{1}{4}F^a_{\mu\nu}F^{a\mu\nu} + \sum_{f=1}^{N_f} \bar{\psi}_f(i\gamma^\mu D_\mu - m_f)\psi_f$$

- Local $SU(3)_c$ gauge invariance.
- Approximate chiral symmetry $SU(N_f)_L \times SU(N_f)_R$ for light quarks; explicitly broken by m_f.
- $U(1)_A$ axial symmetry is broken by the anomaly.
- Symmetry realization changes with T, μ_B, altering spectra, susceptibilities and transport.

Order Parameters: $\langle \bar{q}q \rangle$ and Φ

- Chiral condensate:

$$\langle \bar{q}q \rangle = -\mathrm{Tr}\, S(x,x) = -\int \frac{d^4p}{(2\pi)^4} \mathrm{Tr}\, S(p)$$

drops quickly around T_c.

- Polyakov loop (pure gauge order parameter):

$$\Phi = \frac{1}{N_c} \mathrm{Tr}_c\, \mathcal{P} \exp\left[i \int_0^\beta d\tau\, A_4(\tau, \vec{x}) \right]$$

with $\Phi \approx 0$ (confined) and $\Phi > 0$ (deconfined).

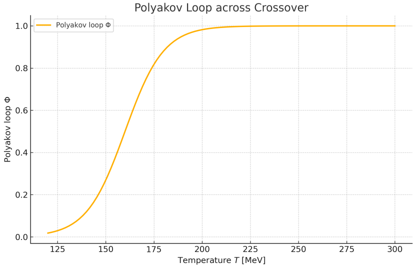

Figure 1: Polyakov loop crossover (lattice inspired).

Thermodynamic Observables from Lattice QCD

- Trace anomaly $\Theta^{\mu}{}_{\mu} = \epsilon - 3P$ peaks near T_c, signaling strong interactions.
- Speed of sound $c_s^2 = \partial P / \partial \epsilon$ exhibits a dip ("softest point").

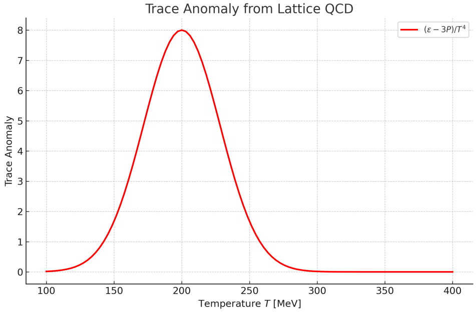

Figure 2: $(\epsilon - 3P)/T^4$ vs T.

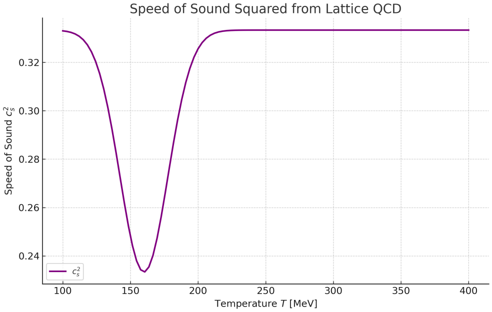

Figure 3: $c_s^2(T)$ minimum near T_c.

Experimental Access to the Phase Diagram

- RHIC/LHC: high T, low μ_B; RHIC BES explores finite μ_B.
- Fluctuations of conserved charges, flow harmonics, dileptons probe phase structure.
- Transport coefficients (η/s, ζ/s) are essential inputs to viscous hydrodynamics.

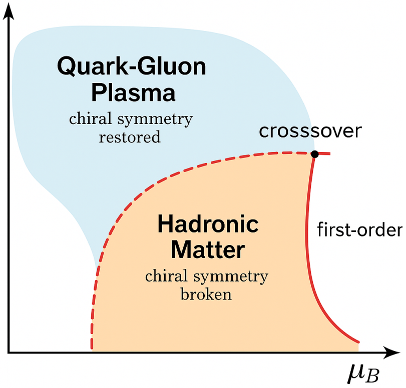

Figure 4: Sketch of QCD phase diagram with crossover, CEP and 1st-order line.

Section Summary

- Chiral and deconfinement transitions intertwine across the (T, μ_B) plane.
- Lattice QCD constrains low-μ_B EOS; effective models extrapolate to higher μ_B.
- Heavy-ion data + transport modeling aim to localize the CEP and constrain the EOS.

Polyakov–Nambu–Jona-Lasinio (PNJL) Model

Lagrangian (Euclidean)

$$\mathcal{L}_{\mathrm{PNJL}} = \bar{q}(i\gamma^{\mu} D_{\mu} - m_0)q + G\left[(\bar{q}q)^2 + (\bar{q}i\gamma^5\vec{\tau}q)^2\right] - \mathcal{U}(\Phi, \bar{\Phi}, T).$$

- G induces SχSB: $M = m_0 - 2G\langle\bar{q}q\rangle$.
- $\mathcal{U}$ mimics (statistical) confinement via $Z(3)$ symmetry.
- Mean-field: quarks couple to a static temporal A_4 background.
- Outputs: $\langle\bar{q}q\rangle$, Φ, EOS and susceptibilities.

Polyakov Potential and Statistical Confinement

$$\frac{\mathcal{U}(\Phi,\bar{\Phi},T)}{T^4} = -\frac{a(T)}{2}\,\bar{\Phi}\Phi + b(T)\ln\left[1 - 6\bar{\Phi}\Phi + 4(\Phi^3+\bar{\Phi}^3) - 3(\bar{\Phi}\Phi)^2\right].$$

- $a(T), b(T)$ fitted to pure-gauge lattice data (reproduce T_c, $Z(3)$ structure).
- Modified Fermi factors $f_\pm$ suppress colored states at low T.

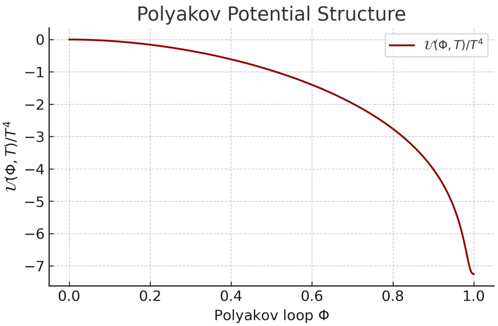

Figure 5: Shape of $\mathcal{U}$ across the crossover.

Thermodynamics in PNJL

$$\Omega(T,\mu_B) = \mathcal{U}(\Phi,\bar{\Phi},T) + \frac{(M-m_0)^2}{4G} - 2N_f N_c \int_0^{\Lambda} \frac{d^3p}{(2\pi)^3} E_p$$
$$- 2TN_f \int \frac{d^3p}{(2\pi)^3} \big[\ln f_+(p) + \ln f_-(p) \big].$$

- Solve $\partial\Omega/\partial M = \partial\Omega/\partial\Phi = \partial\Omega/\partial\bar{\Phi} = 0$.
- EOS: $P = -\Omega$, $s = -\partial\Omega/\partial T$, $n_B = -\partial\Omega/\partial\mu_B$.
- $T_c(\mu_B)$: from inflection points of order parameters; CEP: divergent susceptibilities.

QM/PQM Models and FRG Improvements

(P)QM Lagrangian:

$$\mathcal{L}_{\text{QM}} = \bar{q}(i\gamma^\mu \partial_\mu - g(\sigma + i\gamma_5 \vec{\tau} \cdot \vec{\pi}))q + \mathcal{L}_\sigma, \qquad \text{PQM: add } \mathcal{U}(\Phi, \bar{\Phi}, T).$$

- Mesonic $O(4)$ fields $(\sigma, \vec{\pi})$ encode explicit chiral dynamics and fluctuations.
- Adding the Polyakov loop (PQM) provides statistical confinement.
- FRG: evolve Γ_k to include quantum/thermal fluctuations $\rightarrow$ smoother crossovers, shifted CEP.

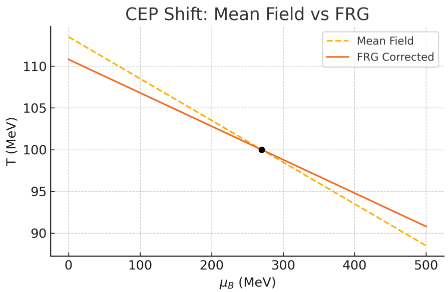

Figure 6: CEP shift: mean-field (black) and FRG (red).

Model Comparison Summary

Model	Chiral	Conf.	Order Params	Pros / Limitations
NJL	✓	×	σ	Simple; analytic; no gluons/Polyakov; no confinement
PNJL	✓	△	σ, Φ	Adds Polyakov loop; semi-quantitative deconfinement; MF artifacts
QM	✓	×	σ (mesonic)	Includes meson fluctuations; quarks unconfined
PQM	✓	△	σ, Φ	Chiral + (de)confinement trends; parameter sensitive
PQM+FRG	✓	△	σ, Φ	Fluctuations via FRG; better CEP; numerically heavy

Table 1: ✓: present; ×: absent; △: approximate/statistical.

AdS/CFT Bounds and Comparison

- KSS bound: $\eta/s \geq 1/4\pi$ in strongly coupled $\mathcal{N}=4$ SYM; PNJL values approach but respect it.
- No strict lower bound for ζ/s; often scales with conformal breaking $(\epsilon - 3P)$ or $(1/3 - c_s^2)$.
- Holographic estimate: $\zeta/\eta \sim (1/3 - c_s^2)$—qualitatively consistent with our trends.

Microscopic Origin of τ_f

- Parametrizations: $\tau_f = C/T$; or $\tau_f = 1/(n\sigma v)$ with n the thermal density and σ an effective cross section.
- pQCD/HTL: at high T, $\tau^{-1} \sim g^4 T \ln(1/g)$; near T_c hadronic/mesonic scatterings dominate.
- Lattice guidance: spectral reconstructions of correlators can constrain rates, but remain challenging.

Kubo Formalism for Viscosity

Retarded correlators

$$\eta = \lim_{\omega\to 0} \frac{1}{20\omega} \int d^4x\, e^{i\omega t}\theta(t)\langle [T_{xy}(x), T_{xy}(0)]\rangle,$$
$$\zeta = \lim_{\omega\to 0} \frac{1}{9\omega} \int d^4x\, e^{i\omega t}\theta(t)\langle [T^{\mu}_{\ \mu}(x), T^{\nu}_{\ \nu}(0)]\rangle.$$

Spectral densities enter via $\mathrm{Im}\, G^R$. Non-perturbative extraction is hard $\Rightarrow$ we resort to kinetic theory / RTA.

Kinetic Theory: Relaxation Time Approximation

$$(\partial_t + \vec{v} \cdot \nabla) f = -\frac{f - f^{(0)}}{\tau_f}, \qquad f^{(0)} = \frac{1}{e^{(E_p - \mu)/T} + 1}.$$

- Linearize: $f = f^{(0)} + \delta f$, solve for δf under shear/bulk perturbations.
- Single τ_f captures microscopic scattering; can depend on T, μ_B, p.
- Use PNJL quasiparticle dispersion $E_p(T, \mu_B)$ for consistency.

Final Expressions for η and ζ

$$\eta(T,\mu_B) = \frac{1}{15T}\int \frac{d^3p}{(2\pi)^3}\frac{p^4}{E_p^2}\,\tau_f f^{(0)}\left[1 - f^{(0)}\right],$$

$$\zeta(T,\mu_B) = \frac{1}{T}\int \frac{d^3p}{(2\pi)^3}\tau_f f^{(0)}\left[1 - f^{(0)}\right]\left(\frac{p^2}{3E_p} - c_s^2 E_p\right)^2.$$

- $c_s^2 = \partial P/\partial\epsilon$ from the PNJL EOS.
- Bulk viscosity is controlled by conformal breaking $(\epsilon - 3P)$ or $(1/3 - c_s^2)$.

Numerical Scheme

- Grid: $T \in [60, 300]$ MeV, $\mu_B \in [0, 600]$ MeV; solve the coupled gap equations point-by-point.
- Momentum integrals: Gauss–Legendre in p (radial) + analytic 4π angular factor; cutoff $p_{\max} \sim 3$ GeV.
- τ_f: choose model (C/T or $1/(n\sigma v)$); test sensitivity.
- Error control: refine p grid until $< 1\%$ variation in η/s, ζ/s.

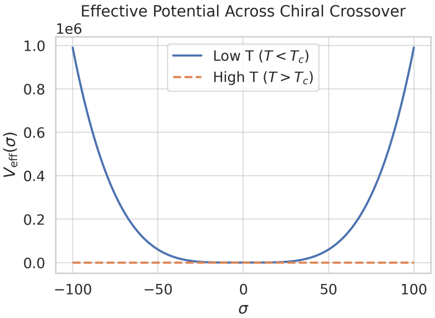

Figure 7: $V_{\text{eff}}(\sigma, T)$ flattens near T_c.

Results: η/s and ζ/s Maps

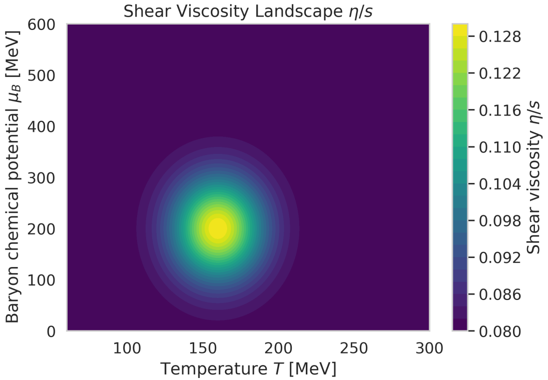

Figure 8: η/s valley along the crossover.

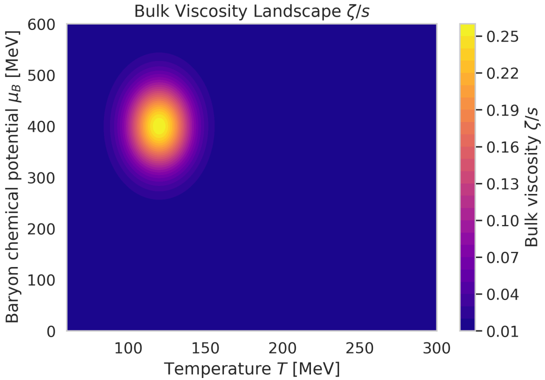

Figure 9: ζ/s peak near the CEP.

- η/s minimized around $T_c(\mu_B) \Rightarrow$ enhanced scattering/collective modes.
- ζ/s enhanced where $c_s^2 \to 0 \Rightarrow$ strong conformal breaking.

Critical Dynamics Interpretation

- Near the CEP, long-range fluctuations (soft modes) drive bulk viscosity up (critical slowing down).
- Shear viscosity dips as scattering off critical modes increases.
- Phenomenology: affects flow fluctuations, higher-order cumulants of conserved charges.

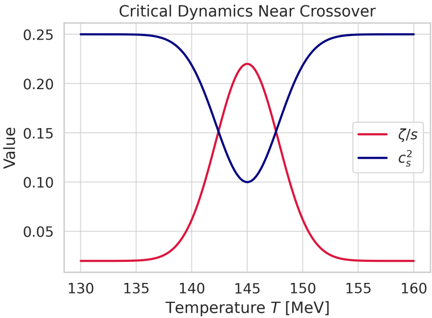

Figure 10: Soft modes boost ζ/s near criticality.

Uncertainties and Sensitivity Analysis

- **Parameter scan**: vary G, Λ, T_0, τ_f model; record shifts in minima/maxima of η/s, ζ/s.
- **Grid convergence**: increase N_p, N_T, N_μ until changes $< 1\%$.
- **Model comparison**: benchmark against lattice-inspired parametrizations or FRG/DSE outputs.
- **Systematics**: choice of Polyakov potential, momentum cutoff, quasiparticle ansatz.

Beyond Viscosity: Other Transport Coefficients

- **Baryon diffusion** D_B and conductivity κ_B: control charge transport near CEP.
- **Electric conductivity** σ_{el}: enters electromagnetic emissivities (photons/dileptons).
- **Thermal conductivity** κ_T: relevant at finite μ_B for heat flow.
- Methods: Kubo formulas for conserved currents, kinetic theory with PNJL quasiparticles, or FRG functional transport.

CEP-sensitive Observables (Heavy-ion Experiments)

- Higher-order cumulants of net-proton/net-charge: $C_4/C_2 = \kappa\sigma^2$, $C_3/C_2 = S\sigma$, etc.
- Non-monotonic energy dependence (RHIC BES-II): search for peak/dip structures vs. $\sqrt{s_{NN}}$.
- Intermittency, scaled factorial moments in transverse-momentum bins.
- Softening signals: directed flow v_1, bulk viscosity imprint on longitudinal decorrelations.
- Dilepton/soft photon rates: sensitive to spectral changes near chiral restoration.

Benchmarking vs Other Approaches

- **FRG/PQM**: compare η/s, ζ/s near CEP (shape and magnitude).
- **Lattice-inspired fits**: EOS, $c_s^2(T)$ at $\mu_B \approx 0$ set baseline.
- **Dyson–Schwinger (DSE)**: transport via Schwinger-Keldysh or memory-function methods.
- Overlay key curves (PNJL vs FRG vs hydro-extracted ranges) to assess robustness.

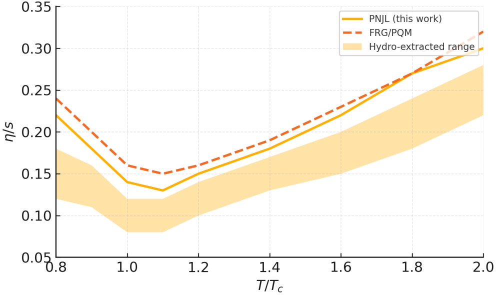

Figure 11: Overlay of $\eta/s(T)$ from different methods.

Effects of Magnetic Field and Vorticity

- Strong B fields in non-central collisions ($eB \sim m_\pi^2$) modify dispersion and scattering $\Rightarrow$ transport anisotropy.
- Chiral Magnetic/Vortical Effects (CME/CVE): induce anomalous currents, alter conductivities.
- Shear viscosity splits into longitudinal/transverse parts in $B \neq 0$; bulk viscosity gains extra terms.
- Vorticity couples to spin degrees of freedom (global polarization), sensitive to relaxation times.

Limitations and Future Work

Model content

- 2-flavor PNJL: no strange quark; extend to 2+1 or full QCD-like Polyakov sector.
- Mean-field artifacts: missing mesonic/critical fluctuations (FRG/DSE can cure partly).

Microscopic inputs

- τ_f is model-dependent; needs kinetic-theory or lattice-informed scattering rates.
- Near the CEP the quasiparticle picture weakens (critical slowing down).

Next steps

- Bayesian model-to-data calibration with heavy-ion observables.
- Event-by-event hydro including critical fluctuations and T, μ_B-dependent transport.
- Couple to astrophysical EOS (NS mergers, cooling) to constrain η, ζ.

Conclusion

- Built a PNJL-based framework to compute η/s and ζ/s on the (T, μ_B) plane.
- Found an η/s valley along the crossover and a ζ/s peak near the CEP.
- These patterns provide guidance for viscous hydrodynamics and CEP searches.
- The setup is extensible: add flavors, FRG fluctuations, and microscopic rates from first principles.

Acknowledgments

- Faculty of Physics, Moscow State University for continuous support.
- GeZhi Theoretical Physics Reading Group for insightful discussions.
- Lanzhou Center for Theoretical Physics for the collaborative environment.
- Thanks to the audience for questions and feedback!
- Endless thanks to my beloved Li Xin, whose support turns every challenge in physics into possibility

Questions and Discussion

Executive Summary (Take-home Messages)

1. η/s hits a minimum, ζ/s spikes near criticality — both trace phase structure.
2. PNJL reproduces lattice trends at low μ_B and extrapolates to finite density.
3. Transport inputs are pivotal for hydrodynamic modeling and CEP searches.
4. Uncertainties stem from τ_f modeling and mean-field limitations.

What's New in This Work

- Joint treatment of chiral restoration and transport in a single PNJL framework.
- Systematic (T, μ_B) scan with consistent gap-equation solutions for M, Φ.
- Combined analysis of η/s *and* ζ/s, highlighting CEP sensitivity.
- Clear road map for upgrading to FRG-based fluctuations and microscopic τ_f.

Astrophysical Relevance

- Bulk viscosity impacts damping of density oscillations in neutron stars / mergers.
- Shear viscosity affects r-mode stability, differential rotation, and thermalization.
- Finite-μ_B transport data inform EOS tables used in multi-messenger simulations.
- Future: interface PNJL/FRG transport with relativistic MHD codes.

Slide Index (Backup Navigation)

Style/Practical Notes (For Presenter)

- Keep ≤ 1 minute per technical slide; dwell longer on result plots.
- Have backup slides ready for τ_f modeling, sensitivity, CEP observables.
- If time-limited: show "Executive Summary" + two key result plots + What's New.

RTA Derivation (Details)

Start from Boltzmann in LR frame:

$$(\partial_t + \vec{v}\cdot\nabla_{\vec{x}})f = C[f], \qquad C[f] \approx -\frac{\delta f}{\tau_f}, \quad f = f^{(0)} + \delta f.$$

Shear perturbation: $u_i(\vec{x})$, $\nabla_{\langle i}u_{j\rangle}$. Project δf onto tensor basis $\sim p_{\langle i}p_{j\rangle}$:

$$\delta f = -\tau_f f^{(0)}(1 - f^{(0)})\,\frac{p_{\langle i}p_{j\rangle}}{2TE_p}\,\nabla_{\langle i}u_{j\rangle}.$$

Insert into T_{ij}, angular average $\Rightarrow$

$$\eta = \frac{1}{15T}\int \frac{d^3p}{(2\pi)^3}\,\frac{p^4}{E_p^2}\,\tau_f f^{(0)}(1 - f^{(0)}).$$

Analogous bulk channel uses $\delta f \propto (\frac{p^2}{3E_p} - c_s^2 E_p)$ giving ζ.

Numerical Workflow (Flowchart)

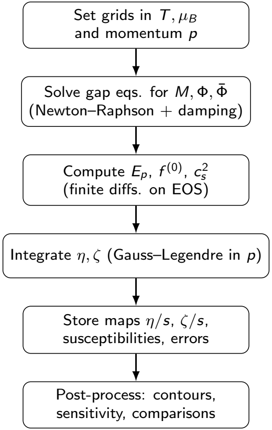

Symbols and Parameters

Symbol	Meaning	Source/Note
T, μ_B	Temperature, baryon chem. pot.	Input grid
$M(T, \mu_B)$	Constituent quark mass	PNJL gap eq.
$\Phi, \bar{\Phi}$	Polyakov loop variables	PNJL potential $\mathcal{U}$
c_s^2	Speed of sound squared	$c_s^2 = \partial P / \partial \epsilon$
τ_f	Relaxation time	Model: C/T or $1/(n\sigma v)$
η, ζ	Shear/Bulk viscosity	RTA integrals (this work)
s	Entropy density	$s = -\partial \Omega / \partial T$
ϵ, P	Energy density, pressure	From PNJL EOS

Kubo for Other Transport Coefficients

- **Baryon conductivity** κ_B: $\kappa_B = -\lim_{\omega\to 0} \frac{1}{\omega} \operatorname{Im} G^R_{J^i_B J^i_B}(\omega, 0)$.
- **Electric conductivity** $\sigma_{\rm el}$: $\sigma_{\rm el} = -\lim_{\omega\to 0} \frac{1}{\omega} \operatorname{Im} G^R_{J^i_{\rm em} J^i_{\rm em}}$.
- **Thermal conductivity** κ_T: via heat current correlator at finite μ_B.

In kinetic theory, replace T_{ij} operator with appropriate current and repeat RTA steps.

Benchmark & Cross-checks

- Compare EOS pieces (P/T^4, ϵ/T^4) with lattice (HotQCD, Wuppertal-Budapest).
- Check η/s minimum $\sim (0.1 - 0.2)$ vs hydro-extracted values from RHIC/LHC.
- Verify ζ/s peak width/height sensitivity to τ_f, c_s^2 parametrization.
- Cross-check CEP location with FRG/PQM and Dyson–Schwinger results.

References I

K. Fukushima, Phys. Lett. B **591**, 277 (2004).

C. Ratti, M. A. Thaler, W. Weise, Phys. Rev. D **73**, 014019 (2006).

P. Kovtun, D. T. Son, A. O. Starinets, Phys. Rev. Lett. **94**, 111601 (2005).

M. A. Stephanov, Phys. Rev. Lett. **102**, 032301 (2009).

A. Bazavov et al., Phys. Rev. D **90**, 094503 (2014).

S. Borsanyi et al., Phys. Lett. B **730**, 99 (2014).

J. E. Bernhard, Ph.D. Thesis, arXiv:1909.04451.

J. Adam et al. (STAR Coll.), Phys. Rev. Lett. **127**, 262301 (2021).

S. Acharya et al. (ALICE Coll.), Phys. Rev. Lett. **123**, 142301 (2019).

F. Karsch, D. Kharzeev, K. Tuchin, Phys. Lett. B **663**, 217 (2008).

J. Noronha-Hostler, J. Noronha, C. Greiner, Phys. Rev. C **89**, 054904 (2014).

J.-B. Rose et al., Nucl. Phys. A **928**, 51 (2018).

R.-A. Tripolt et al., Phys. Rev. D **97**, 034022 (2018).

R. Critelli et al., Phys. Rev. D **96**, 096026 (2017).

References II

- F. Karsch, K. Redlich, Phys. Rev. D **93**, 114517 (2016).
- J. M. Pawlowski, N. Strodthoff, Phys. Rev. D **92**, 094009 (2015).
- J. Grefa et al., Phys. Rev. C **104**, 064903 (2021).
- X. An, G. Basar, M. Stephanov, H.-U. Yee, Phys. Rev. C **100**, 024910 (2019).
- B. Singh et al., Phys. Rev. D **106**, 014015 (2022).
- W.-j. Fu, J. M. Pawlowski, F. Rennecke, Phys. Rev. D **101**, 054032 (2020).
- M. Bluhm, B. Kämpfer, K. Redlich, Eur. Phys. J. C **80**, 333 (2020).
- A. Monnai, Phys. Rev. C **96**, 044909 (2017).
- C. Ratti, Rept. Prog. Phys. **81**, 084301 (2018).
- T. Dore et al., Phys. Rev. D **102**, 096017 (2020).
- D. Almaalol, J. Noronha-Hostler, Phys. Rev. C **106**, 014912 (2022).
- M. Nahrgang et al., Phys. Rev. C **101**, 014902 (2020).
- B. Schenke et al., Phys. Rev. Lett. **125**, 142301 (2020).
- A. Kurkela et al., Phys. Rev. Lett. **128**, 102701 (2022).

References III